Journal of Nanofluids
Vol. 10, pp. 75–82, 2021
(www.aspbs.com/jon)

Significance of Magnetic Field on Carreau Dissipative Flow Over a Curved Porous Surface with Activation Energy

Gadamsetty Revathi[1], Jayachandra Babu Macherla[2], Chakravarthula Sivakrishnam Raju[3,*], Rohit Sharma[3], and Ali J. Chamkha[4]

[1] *Department of Mathematics, Gokaraju Rangaraju Institute of Engineering and Technology, Bachupally 500090, Hyderabad, India*
[2] *Department of Mathematics, S.V.A Govt. College, Srikalahasti 517644, India*
[3] *Department of Mathematics, GITAM University, Bangalore 562163, Karnataka, India*
[4] *Faculty of Engineering, Kuwait College of Science and Technology, Doha District, 35004 Kuwait*

This paper theoretically clarifies the impact of pertinent parameters, including viscous dissipation on the flow of Carreau fluid through a permeable arched elongating sheet. Flow describing equations are metamorphosed as ODEs and executed using the combination of shooting and Runge-Kutta strategies. Consequences are elucidated using tables and graphs. We discovered that (a) an appreciable decline in the concentration against temperature difference and reaction rate parameters (b) curvature parameter and porosity parameters registered opposite behaviour to each other on velocity profile (c) there is a reduction in the heat transfer rate with larger Eckert number and curvature parameters (d) Biot number ameliorates the temperature and local Nusselt number (e) Schmidt number and activation energy parameters are showing different behaviours on local Sherwood number. And also, magnetic field and porosity parameters minimize the velocity and surface drag force and Biot number ameliorates the temperature. Further, present results are validated with the earlier outcomes and perceived an acceptable agreement.

KEYWORDS: Carreau Fluid, Curved Stretching Sheet, Shooting Procedure, Curvature Parameter, Porosity Parameter, Activation Energy Parameter.

1. INTRODUCTION

Extrusion is a process in the industries, dealing with materials including polymers, plastics. In recent times, extrusion cooking has become a significant food processing activity. The greater part of the pertinent materials in these procedures are non-Newtonian, with a shear rate reliant on viscosity, and hence carry on considerably not quite the same as Newtonian fluids, for example, air and water. The word "non-Newtonian" is an exceptionally wide one which envelope an enormous assortment of fluids with basically dissimilar rheological features. Blood, ketchup, paint, jams, palm oil are a few instances of non-Newtonian fluids. Non-Newtonian fluids have been exposed to numerous investigations regarding the energy transport and forecast of drag force over 50 years. This is due to the expanded use of non-Newtonian fluids in the industry, with examples including molten plastics and pulps, which are ultimately propelled in factories analogous to usual Newtonian fluids. Sarpkaya[1] started the work on the non-Newtonian fluid flow amongst two parallel planes with magnetic field. Tomita[2] obtained the relation among the Reynolds number and the boundary layer thickness after applying the boundary layer theory concept to the non-Newtonian fluid flow at the high Reynold's number. Huang[3] presented numerical solutions for the laminar non-Newtonian flow through a porous annulus with the aid of perturbation and quasi-linearization methods. Chandrupatla and Sastri[4] and Hanks and Larsen[5] demonstrated power-law fluid flows over different geometries. One of their discoveries is, pseudoplastic fluids are superior functioning fluids in heat exchange apparatus than Newtonian fluids. Rajagopal et al.[6] analysed the behaviour of skin friction in different situations in the examination of Falkner-Skan flow across a wedge. Chaoyang and Chuanjing[7] explained the heat transfer characteristics of non-Newtonian fluid flow in two cases (natural and forced convection) in porous media. Prasad et al.[8] considered elongating sheet as a geometry and elucidated

*Author to whom correspondence should be addressed.
Emails: rchakrav@gitam.edu, sivaphd90@gmail.com
Received: 12 April 2021
Accepted: 11 May 2021

ARTICLE

the visco-elastic flow. They remarked that the visco-elastic parameter escalates the mass transfer rate. Xu and Liao[9] applied HAM to provide the outcomes for the MHD non-Newtonian fluid flow triggered via an impulsively stretching plate. By considering stretching sheet, several researchers[10–13] scrutinized distinct non-Newtonian fluid flows. Their findings include a point that the entropy generation function upsurges up to a firm distance from the sheet with the rise in the magnetic parameter. Santhosh and Raju[14–15] considered exponential stretching sheet and scrutinized different Carreau fluid flows with various parameters including thermal radiation. Later, Maleki et al.[16] elucidated the non-Newtonian nanofluid flow through a porous surface and observed that for injection and suction cases, the utilization of nanoparticles does not significantly affect heat transfer. Further, some authors[17–22] deliberated diverse non-Newtonian fluid flows over different geometries. Khan et al.[23] elucidated Carreau fluid flow with Cattaneo-Christov heat flux by a shrinking/stretching cylinder. They observed an escalation in the surface drag forice with larger magnetic field parameter. Madhu et al.[24] used FEM (Finite Element Method) to resolve the mathematical model to examine the Carreau fluid flow in an inclined microchannel with entropy generation optimization. They detected the reduction in the entropy generation at the right and left phase of the channel. Recently, various researchers[25–27] considered distinct geometries and inspected Carreau fluid flow with Joule heating as one of the parameter.

The stretching sheet is utilized for polymer expulsion procedures, which is prepared with the mixture of both polymer sheets and metal. By considering stretching surface as a geometry, several researchers analysed the characteristics of heat transfer and flow because of its extensive scope of uses in engineering and industries problems. Instances of such procedures regarding polymers incorporate cooling of filaments, glass blowing, synthetic fibers, hot rolling and so forth. In all the procedures referenced above, the final product relies upon the rate of heat transfer and surface drag force at the surface. In 1961, Sakiadis[28] provided the boundary layer equations of motion for laminar flow on a continuous solid surface. This work was extended by Crane[29] to a stretching sheet in 1970, who solved energy equation with various values of Prandtl number. Gupta and Gupta[30] considered the same geometry and elucidated the features of two transports (heat, mass) of the flow. They perceived that the temperature declines with the rise in blowing. Hassanien and Gorla[31] used generalised Newton's method to explain the influence of several parameters on the common profiles in the inspection of micropolar fluid flow through an elongating sheet. Majeed et al.[32] discovered that the Prandtl number lowers the temperature in the analysis of ferromagnetic viscoelastic flow. Hussain et al.[33] mentioned that, contrast with fluid parameter, magnetic field parameter impact is progressively noticeable on local shear stress. Shah et al.[34] explored the Williamson fluid flow by a permeable elongating sheet. By considering heat source/sink and elongating sheet, Hosseinzadeh et al.[35] numerically scrutinised the nanofluid flow. Later several researchers[36–44] explained different MHD fluid flows over a stretching sheet with several parameters including Peclet number. In all the above examinations, the stretching sheet is viewed as flat, and mathematical modelling is completed utilizing cartesian coordinates. But, one can complete the same modelling by obtaining the governing equations with the aid of curvilinear coordinates system, when curved stretched sheet is considered. Flow over a curved stretching sheet has gained ample influences in the examination of boundary layer flow because of its amazing importance in engineering and manufacturing segments, for example, making of paper crafts, wire drawing, rubber sheets manufacturing, and so forth. Rosca and Pop[45] performed a numerical study on the viscid flow through a permeable arched contracting/elongating sheet and discovered that the suction parameter upsurges the shrinking parameter. Naveed et al.[46–47] deliberated different flows across the same geometry and witnessed that the material parameter exhibit different behaviour on fluid temperature and velocity. Imtiaz et al.[48] provided convergent series solutions to discuss the outcomes of their work and found that the curvature parameter raises the temperature. Recently, Kumar et al.[49] and Taseer et al.[50] explained different fluid flows across a curved stretching sheet with several parameters, including thermal radiation.

From the above conversation, it is completely clear that the impression of activation energy parameter on Carreau fluid flow through an arched elongating sheet with viscous dissipation and Schmidt number is not explored up until this point. In this manner, the goal of the present work is to make such an endeavour. Numerical solution of the problem is gotten by utilizing the combination of Runge-Kutta and shooting strategies. Results are disclosed via plots and table in two cases. To approve the precision of our investigation, an examination is made with the past work by Ahmad et al.[51] and all outcomes are found in acceptable agreement.

2. FORMULATION

A steady, incompressible 2D Carreau fluid flow across a arched elongating sheet. Elongated velocity of the sheet is denoted by $u_w = ds$. Arched elongating sheet is nestled in a circle or radius R. B_0 is the intensity of the magnetic field, which is enforced in r-direction. It is presumed that C_∞ and C_w designate the ambient and surface concentration while T_∞ and T_w designate the ambient and surface temperatures respectively. Flow geometry is presented in Figure 1.

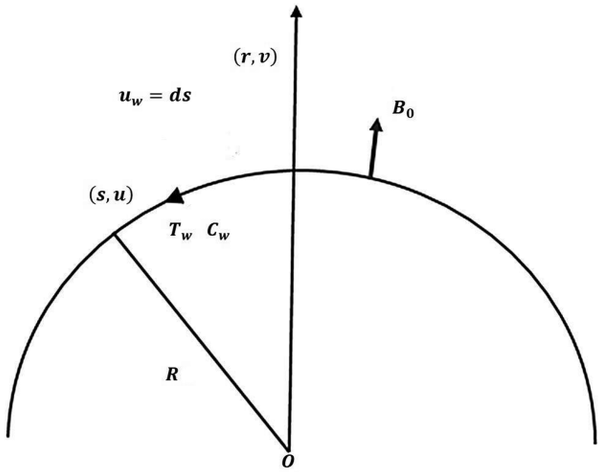

Fig. 1. Flow geometry of the present problem.

With these presumptions, flow driven equations are given as:[47]

$$\frac{\partial}{\partial r}\left[v\left(R+r\right)\right]+\frac{\partial u}{\partial s}R=0 \tag{1}$$

$$u\frac{u}{R+r}=\frac{\partial}{\partial r}\left(\frac{p}{\rho}\right) \tag{2}$$

$$\begin{aligned}&\rho\left(\frac{\partial u}{\partial r}v+\frac{\partial u}{\partial s}\frac{u}{R+r}R+\frac{vu}{R+r}\right)\\&=-\frac{\partial P}{\partial s}\frac{R}{R+r}+\mu\left(\frac{\partial^2 u}{\partial r^2}+\frac{\partial u}{\partial r}\frac{1}{R+r}-\frac{1}{R+r}\frac{u}{R+r}\right)\\&\times\left[1+\Gamma^2\frac{\partial u}{\partial r}\frac{\partial u}{\partial r}\right]^{(n-1)/2}+\mu\left(\frac{\partial^2 u}{\partial r^2}+\frac{\partial u}{\partial r}\frac{1}{R+r}\right.\\&\left.-\frac{1}{R+r}\frac{u}{R+r}\right)\Gamma^2\left(n-1\right)\left(\frac{\partial u}{\partial r}\right)^2\\&\times\left[1+\Gamma^2\frac{\partial u}{\partial r}\frac{\partial u}{\partial r}\right]^{(n-3)/2}-\sigma B_0^2 u-\frac{u}{\kappa}\mu\end{aligned} \tag{3}$$

$$\begin{aligned}v\frac{\partial T}{\partial r}+\frac{1}{R+r}Ru\frac{\partial T}{\partial s}&=\frac{k}{\rho C_p}\left(\frac{\partial^2 T}{\partial r^2}+\frac{\partial T}{\partial r}\frac{1}{r+R}\right)\\&+\frac{v}{C_p}\left(\frac{\partial u}{\partial r}\right)^2\end{aligned} \tag{4}$$

$$\begin{aligned}v\frac{\partial C}{\partial r}+\frac{R}{r+R}u\frac{\partial C}{\partial s}&=D_m\left(\frac{\partial^2 C}{\partial r^2}+\frac{1}{r+R}\frac{\partial C}{\partial r}\right)\\&-k_1^2\left(\frac{T}{T_\infty}\right)^m\exp\left(-\frac{E_1}{k*T}\right)\\&\times\left(C-C_\infty\right)\end{aligned} \tag{5}$$

with the conditions

$$\left.\begin{gathered}u\left(0,s\right)=u_w,\quad v(0,s)=0,\\-k\frac{\partial T}{\partial r}\Big|_{r=0}=h\left(T_w-T\right),\quad \mathrm{C}\left(0,s\right)=C_w\\u\left(r,s\right)\to 0,\quad \frac{\partial u\left(r,s\right)}{\partial r}\to 0,\quad T\left(r,s\right)\to T_\infty,\\C\left(r,s\right)\to C_\infty\quad \text{as}\quad r\to\infty\end{gathered}\right\} \tag{6}$$

Here u component of velocity in s direction, v component of velocity in r direction, n power law index parameter, m fitted rate constant , $k*$ Boltzmann constant, σ electrical conductivity, υ kinematic viscosity, ρ fluid density, κ permeability of the porous medium, Γ fluid relaxation time, T fluid temperature, C_p specific heat capacitance, k thermal conductivity, C fluid concentration, k_1 chemical reaction rate, D_m molecular diffusivity, E_1 activation energy parameter, h convective heat transfer coefficient.

With the transmutations[47]

$$\left.\begin{gathered}\eta=\sqrt{\frac{u_w}{\upsilon s}}r,\quad p=\rho d^2 s^2 P\left(\eta\right),\quad u=dsf'\left(\eta\right),\\v=-\frac{R}{r+R}\sqrt{d\upsilon}f\left(\eta\right),\\T=\left(-T_\infty+T_w\right)\theta(\eta)+T_\infty,\\C=\left(-C_\infty+C_w\right)\phi(\eta)+C_\infty\end{gathered}\right\} \tag{7}$$

Eq. (1) is trivially satisfied, the Eqs. (2)–(5) metamorphosed as:

$$\frac{dP}{d\eta}=\frac{f'^2}{\eta+K} \tag{8}$$

$$\begin{aligned}\frac{2K}{\eta+K}P&=\left(f'''+\frac{1}{\eta+K}f''\right)\left(1+We^2 f''^2\right)^{(n-3)/2}\\&\times\left(1+nWe^2 f''^2\right)+\frac{K}{\eta+K}\left(ff''-f'^2\right.\\&\left.+\frac{1}{\eta+K}ff'\right)-\frac{1}{\left(\eta+K\right)^2}f'\\&-\left(M+\lambda\right)f'\end{aligned} \tag{9}$$

$$\theta''+\frac{K}{\eta+K}\Pr f\theta'+\frac{\theta'}{\eta+K}+\Pr Ecf''^2=0 \tag{10}$$

$$\begin{aligned}\phi''+\frac{K}{\eta+K}Scf\phi'+\frac{\phi'}{\eta+K}-Sc\Lambda\left(1+\gamma\theta\right)^m\\\times\exp\left(-\frac{E}{1+\gamma\theta}\right)\phi=0\end{aligned} \tag{11}$$

ARTICLE

and conditions (6) metamorphosed as

$$\left.\begin{aligned} & f(\eta)=0, \quad \left.\frac{df}{d\eta}\right|_{\eta=0}=1, \\ & \left.\frac{d\theta}{d\eta}\right|_{\eta=0}=-(1-\theta(\eta))\,Bi, \\ & \phi(\eta)=1 \quad \text{at} \quad \eta=0 \\ & \frac{df}{d\eta}\to 0, \quad \frac{d^2 f}{d\eta^2}\to 0, \quad \theta(\eta)\to 0, \\ & \phi(\eta)\to 0 \quad \text{as} \quad \eta\to\infty \end{aligned}\right\} \tag{12}$$

Curvature parameter K, Weissenberg parameter We, porosity parameter λ, Prandtl number Pr, Schmidt number Sc, temperature difference parameter γ, Eckert number Ec, reaction rate parameter Λ, activation energy parameter E, magnetic field parameter M, Biot number Bi are designed as:

$$\left.\begin{aligned} & K=R\sqrt{\frac{d}{\upsilon}}, \quad We=\sqrt{\frac{\Gamma^2 d u_w^2}{\upsilon}}, \quad \lambda=\frac{\upsilon}{\kappa d}, \\ & Pr=\frac{\mu C_p}{k}, \quad Sc=\frac{\upsilon}{D_m}, \quad \gamma=\frac{T_w-T_\infty}{T_\infty}, \\ & Ec=\frac{{u_w}^2}{C_p(T_w-T_\infty)}, \quad \Lambda=\frac{{k_1}^2}{d}, \quad E=\frac{E_1}{k*T_\infty}, \\ & M=\frac{\sigma {B_0}^2}{\rho d}, \quad Bi=\frac{h\sqrt{\frac{\upsilon}{d}}}{k} \end{aligned}\right\} \tag{13}$$

With the help of Eq. (9), Eq. (8) can be rewritten as

$$\begin{aligned} & [1+We^2 f''^2]^{(n-3)/2}[1+nWe^2 f''^2]f^{iv}+[1+We^2 f''^2] \\ & \times[1+nWe^2 f''^2]\frac{2f'''}{\eta+K}+[1+f''^2 We^2]^{(n-5)*0.5}(n-3) \\ & \times[1+f''^2 We^2 n]f'' We^2 f'''\left(f'''+f''\frac{1}{K+\eta}\right) \\ & -\frac{1}{K+\eta}\frac{f''}{K+\eta}+\frac{1}{(K+\eta)^2}\frac{f'}{(K+\eta)}-\frac{1}{K+\eta} \\ & \times(f''f'-f'''f)K-\frac{1}{(K+\eta)}(-ff''+f'^2)\frac{K}{K+\eta} \\ & -\frac{K}{K+\eta}ff'\frac{1}{(\eta+K)^2}-(M+\lambda) \\ & \times\left(f''+\frac{f'}{\eta+K}\right)=0 \end{aligned} \tag{14}$$

Surface drag force C_{fs}, Sherwood number Sh_s, Nusselt numbers Nu_s are characterized as (Naveed et al. [46])

$$C_{fs}=\frac{\tau_{rs}}{\rho u_w^2}, \quad Sh_s=\frac{sj_w}{D_m(C_w-C_\infty)},$$
$$Nu_s=\frac{sq_w}{k(T_w-T_\infty)} \tag{15}$$

[τ_{rs} (wall shear stress), j_w (heat flux) and q_w (heat flux) are specified as

$$\tau_{rs}=\mu\left(\left[1+\Gamma^2\left(\frac{\partial u}{\partial r}\right)^2\right]^{(n-1)/2}\frac{\partial u}{\partial r}-\frac{u}{R+r}\right)\Bigg|_{r=0},$$
$$j_w=-\left(\frac{\partial C}{\partial r}\right)D_m\Bigg|_{r=0}, \quad q_w=-\left(\frac{\partial T}{\partial r}\right)k\Bigg|_{r=0}\ ] \tag{16}$$

and their non-dimensional forms are designated as:

$$\left.\begin{aligned} & (Re_s)^{1/2}C_{fs}=\left[1+(f''(\eta))^2 We^2\right]^{(n-1)*0.5} \\ & \qquad\times f''(\eta)-f'(\eta)\frac{1}{K}\,|_{\eta=0}, \\ & (Re_s)^{-1/2}Sh_s=-\phi'(\eta)|_{\eta=0}, \\ & (Re_s)^{-1/2}Nu_s=-\theta'(\eta)|_{\eta=0} \end{aligned}\right\} \tag{17}$$

where $Re_s=(su_w)/\upsilon$ (Reynold's number).

3. DISCUSSION

Equations (10)–(11), (15) with conditions (12) are puzzled out numerically by executing the combination of Runge-Kutta and shooting strategies by taking $K=2$, $Sc=0.6$, $n=0.5$, $\lambda=0.5$, $Ec=0.3$, $\Lambda=1.5$, $\gamma=0.1$, $Pr=0.71$, $m=0.5$, $E=0.5$, $M=1.5$, $Bi=0.5$. Consequences are elucidated by plots and tables in two cases i.e., $We=0.5$ and $We=0$. In both cases, we witnessed the same impact (increasing or decreasing).

3.1. Concentration Profile

It is witnessed from Figure 2 that larger Sc minimizes the fluid concentration. Typically, escalation in Sc leads to the deceleration in mass diffusivity of the fluid. Figure 3 affirms that E ameliorates fluid concentration. From Figure 4, it is emphasized that larger Λ minimizes the concentration. It is noticed that profiles are

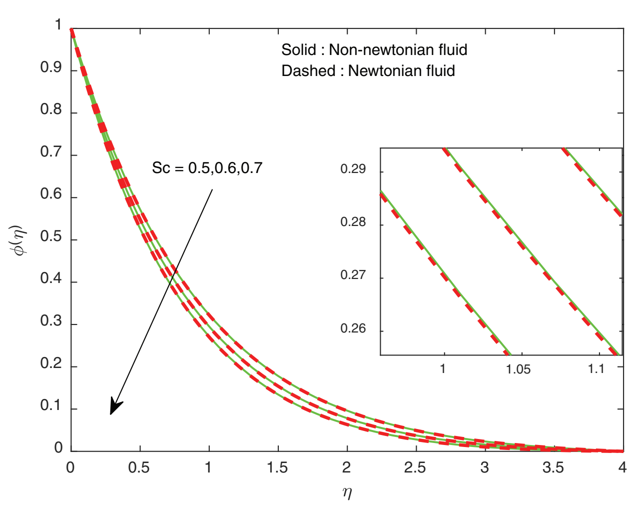

Fig. 2. Outcome of Sc on concentration.

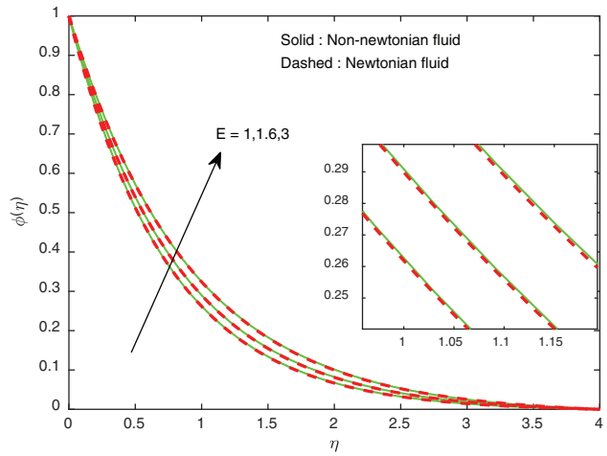

Fig. 3. Outcome of E on concentration.

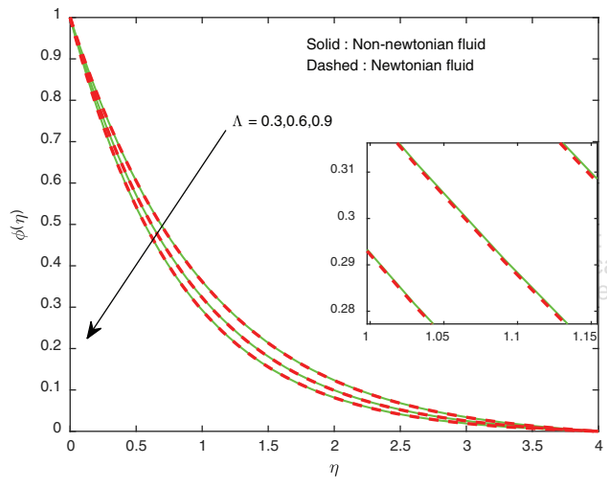

Fig. 4. Outcome of Λ on concentration.

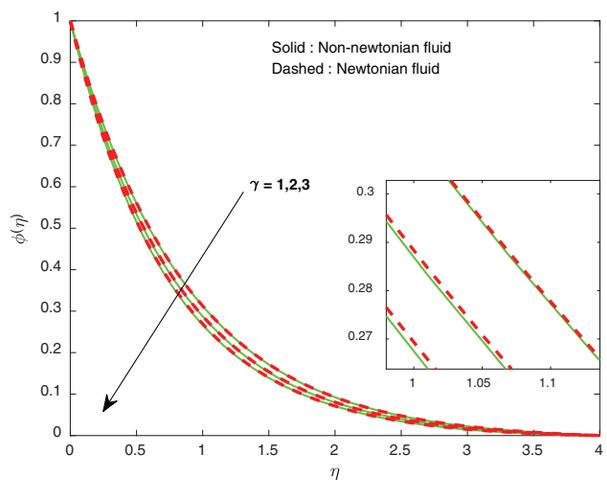

Fig. 5. Outcome of γ on concentration.

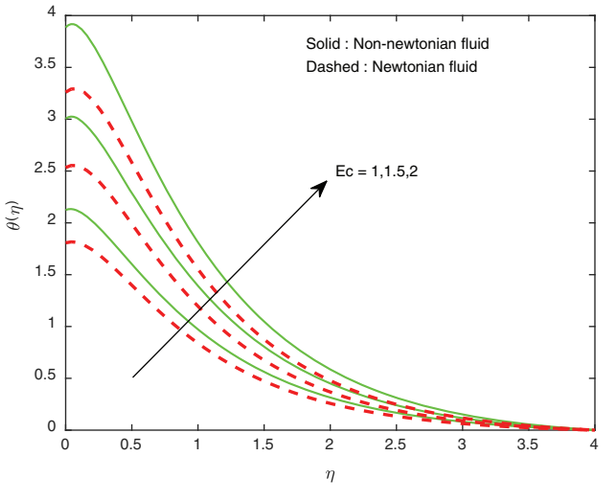

Fig. 6. Outcome of Ec on temperature.

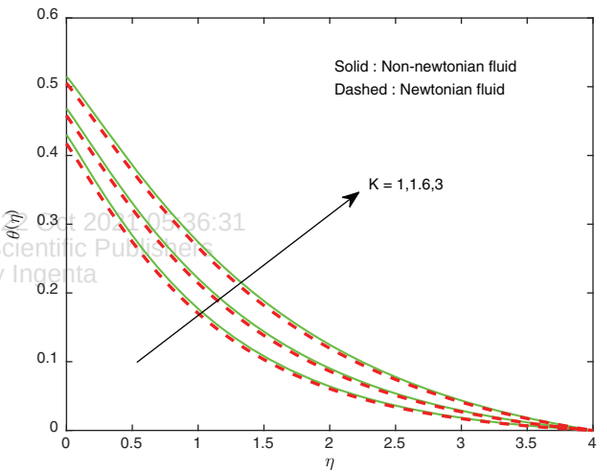

Fig. 7. Outcome of K on temperature.

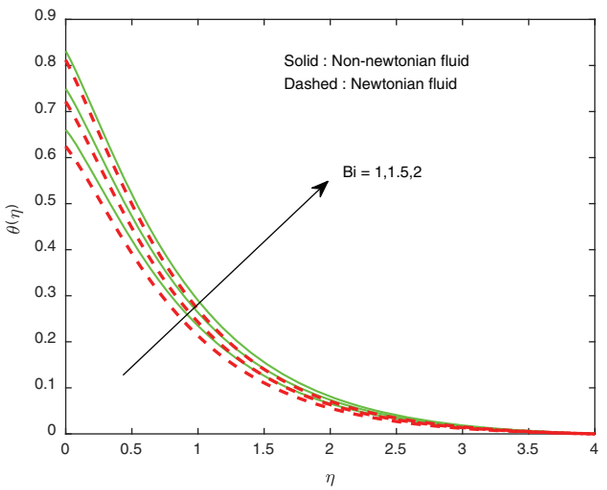

Fig. 8. Outcome of Bi on temperature.

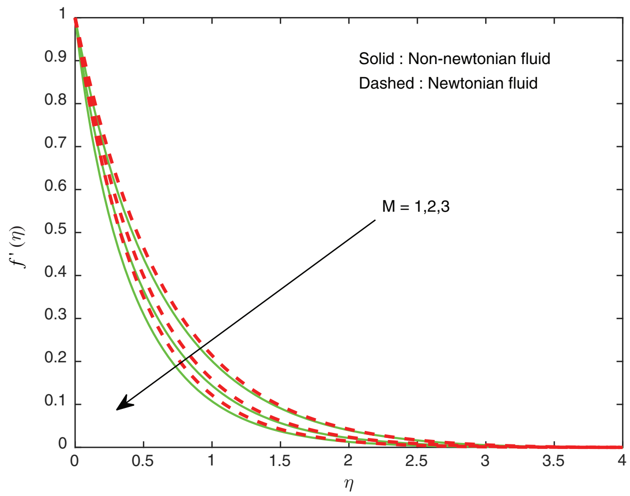

Fig. 9. Outcome of M on velocity.

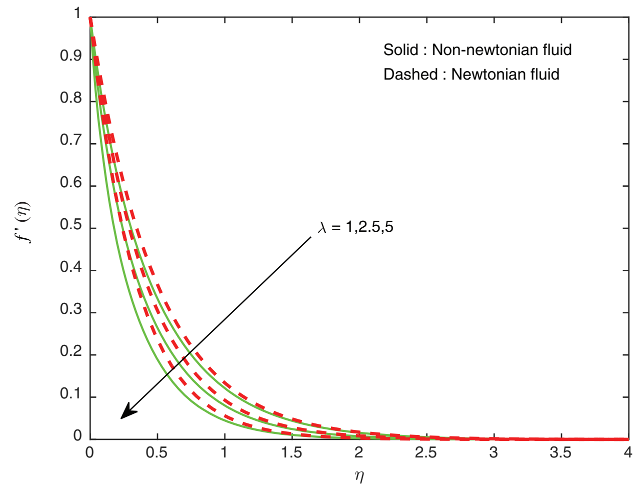

Fig. 11. Outcome of λ on velocity.

appearing predominant in the case of $We = 0.5$ compared to the other. Figure 5 affirms that γ lowers the same (concentration).

3.2. Temperature Profile

Eckert number initiate the action of transmutation of shear forces into heat, which affirms the result in Figure 6 (increment). Note that, there is an increase in the radius of the surface with the raise in K. So, thickness of the thermal boundary layer ameliorates, which in turn, aid to enhance the temperature (Fig. 7). Figure 8 reported that Bi intensify the temperature. Typically, quantity of heat transferred to the fluid flow escalates with the larger Biot number.

3.3. Velocity Profile

Due to Lorentz force (which arises owing to the transfer of energy among electric and magnetic fields during the movement of fluid), there is an escalation of the resistance to the flow. So, M minimizes the velocity (Fig. 9). Figure 10 enlightens the change in velocity with curvature parameter. Surface radius becomes higher with the escalation in K. So, fluid velocity ameliorates. Step-up in porosity parameter (λ) leads to the creation of large amount of porous spaces, which offers more resistance to the flow. Figure 11 affirms the same. We detected that profiles are appearing more prominent in case of Newtonian fluid.

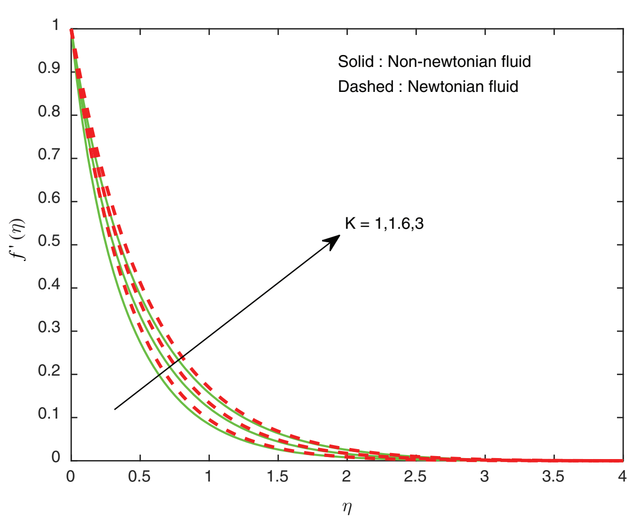

Fig. 10. Outcome of K on velocity.

Table I. Numerical values of surface drag force for different parameters.

			$Re_s^{0.5} C_{fs}$	
M	K	λ	Non-newtonian fluid	Newtonian fluid
1			−2.033689	−2.027294
2			−2.366173	−2.336660
3			−2.668236	−2.601716
	1		−3.326969	−3.329360
	1.6		−2.619560	−2.630139
	3		−2.108216	−2.102186
		1	−2.517283	−2.507122
		2.5	−2.952692	−2.877835
		5	−3.670820	−3.388083

Table II. Values of heat transfer rate for various parameters.

			$Re_s^{-0.5} Nu_s$	
Ec	K	Bi	Non-newtonian fluid	Newtonian fluid
1			−0.561973	−0.403660
1.5			−1.002414	−0.766904
2			−1.442856	−1.130162
	1		0.284893	0.291394
	1.6		0.265666	0.270980
	3		0.242414	0.247375
		1	0.339792	0.375680
		1.7	0.426244	0.473511
		3	0.505929	0.564515

Table III. Values of mass transfer rate for various parameters.

E	Λ	Sc	γ	$Re_s^{-0.5} Sh_s$	
				Non-newtonian fluid	Newtonian fluid
1				1.332499	1.332984
1.6				1.228297	1.229217
3				1.108869	1.110796
	0.3			0.992120	0.992695
	0.6			1.109992	1.109990
	0.9			1.213103	1.212626
		0.5		1.099404	1.099640
		0.6		1.180963	1.181203
		0.7		1.256366	1.256603
			1	1.153483	1.148888
			2	1.255083	1.247237
			3	1.337163	1.327150

Table IV. Validation of present results with the previous results for skin friction.

K	M	λ	$-Re_s^{0.5} C_{f_s}$ (skin friction)	
			Ahmad et al.[51]	Present study
5	0.2	0.5	1.53300	1.533000
10			1.41300	1.413000
20			1.35700	1.357000
10	0	0.5	1.32800	1.328000
	0.2		1.41300	1.413000
	0.4		1.49300	1.493000

From Table I, it is understandable that porosity and magnetic field parameters are decreasing functions of surface drag force in contrast to curvature parameter. Table II clarifies that Eckert number and curvature parameters minimize the local Nusselt number but Biot number step-up the same. Table III elucidate that Schmidt number, temperature difference parameter and reaction rate parameters are having the same impact (raise) on local Sherwood number in contrast to activation energy parameter. Table IV displays the correlation among the present outcomes and the previous outcomes (for the numerical estimations of friction factor). We found a respectable understanding. This decides the aptness of the present investigation.

4. CONCLUSION

A theoretical investigation is designed to observe the impact of several parameters, for instance, viscous dissipation on Carreau fluid flow through an arched elongating sheet. We used the combination of Runge-Kutta and shooting techniques to solve the metamorphosed equations. Results are explained through tables and plots. Outcomes are validated with the earlier results and noticed an acceptable accord. The principal deductions of the current problem are drawn as follows:

- Magnetic field minimizes the velocity and surface drag force.
- An appreciable decline has been noticed in the concentration against temperature difference and reaction rate parameters.
- Temperature ameliorates with larger Eckert number.
- Activation energy parameter enriches fluid concentration.
- Curvature parameter and porosity parameters registered opposite behaviour to each other on velocity profile.
- Porosity parameter minimizes the surface drag force.
- Observed shrink in the heat transfer rate with larger Ec and K.
- Biot number ameliorates the temperature and local Nusselt number.
- Eckert number lessens the heat transfer rate.
- Schmidt number and activation energy parameters are showing different behaviours on local Sherwood number.

References and Notes

1. T. Sarpkaya, *A. I. Ch. E. J.* 7, 324 (**1961**).
2. Y. Tomita, *Bulletin of JSME* 4, 77 (**1961**).
3. C. L. Huang, *J. Math. Anal. Appl.* 59, 130 (**1977**).
4. R. C. Ashok and V. M. K. Sastri, *Numer. Heat Transf. Part B: Fundaments: An Int. J. Comp. Methodology* 1, 243 (**1978**).
5. R. W. Hanks and K. M. Larsen, *Ind. Eng. Chem. Fundam.* 18, 33 (**1979**).
6. K. R. Rajagopal, A. S. Gupta, and T. Y. Na, *Int. J. Non-Linear Mechanics* 18, 313 (**1983**).
7. W. Chaoyang and T. Chuanjing, *Int. J. Heat Fluid Flow* 10, 160 (**1989**).
8. K. V. Prasad, S. Abel, and P. S. Datti, *Int. J. Non-Linear Mech.* 38, 651 (**2003**).
9. H. Xu and S. Liao, *J. Non-Newtonian Fluid Mech.* 129, 46 (**2005**).
10. T. Javed, N. Ali, Z. Abbas, and M. Sajid, *Chemical Eng. Commun.* 200, 327 (**2013**).
11. S. Nadeem, R. U. Haq, N. S. Akbar, and Z. H. Khan, *Alexandria Eng. J.* 52, 577 (**2013**).
12. M. M. Rashidi, S. Bagheri, E. Momoniat, and N. Freidoonimehr, *Ain Shams Eng. J.* 8, 77 (**2017**).
13. M. Jayachandra Babu and N. Sandeep, *Alexandria Eng. J.* 55, 2193 (**2016**).
14. H. B. Santhosh and C. S. K. Raju, *Journal of Nanofluids* 7, 72 (**2018**).
15. H. B. Santhosh and C. S. K. Raju, *Journal of Nanofluids* 7, 1130 (**2018**).
16. H. Maleki, M. R. Safaei, A. A. A. A. Alreashed, and A. Kasaeian, *J. Thermal Anal. Calorimetry* 135, 1655 (**2019**).
17. A. Hussain, S. Akbar, L. Sarwar, S. Nadeem, and Z. Iqbal, *Heliyon* 5, e01203 (**2019**).
18. S. M. Atif, S. Hussain, and M. Sagheer, *Journal of Nanofluids* 8, 806 (**2019**).
19. A. Ghasemian, S. Dinarvand, A. Adamian, and M. A. Sheremet, *Journal of Nanofluids* 8, 1544 (**2019**).
20. M. I. Khan, M. Nigar, T. Hayat, and A. Alsaedi, *Computer Methods and Programs in Biomedicine* 187, 105221 (**2020**).
21. P. Renuka, B. Ganga, R. Kalaivanan, and A. K. Abdul Hakeem, *J. Appl. Comput. Mech.* 6, 296 (**2020**).
22. H. A. Nabwey, *Journal of Nanofluids* 9, 121 (**2020**).
23. M. I. Khan, M. Nigar, T. Hayat, A. Alsaedi, *Computer Methods and Programs in Biomedicine* 187, 105221 (**2020**).
24. M. Madhu, B. Mahanthesh, N. S. Shashikumar, S. A. Shehzad, S. U. Khan, and B. J. Gireesha, *International Communications in Heat and Mass Transfer* 117, 104761 (**2020**).

25. M. M. Bhatti, L. Phali, and C. M. Khalique, *Archive of Applied Mechanics* 91, 1683 **(2021)**.
26. T. Hayat, F. Haider, A. Alsaedi, and B. Ahmad, *International Communications in Heat and Mass Transfer* 120, 105073 **(2021)**.
27. S. A. Shehzad, M. Madhu, N. S. Shashikumar, B. J. Gireesha, and B. Mahanthesh, *Journal of Thermal Analysis and Calorimetry* 143, 2717 **(2021)**.
28. B. C. Sakiadis, *AIChE J.* 7, 26 **(1961)**.
29. L. J. Crane, *J. Appl. Math. Phys.* 21, 645 **(1970)**.
30. P. S. Gupta and A. S. Gupta, *Canad. J. Chem. Eng.* 55, 744 **(1977)**.
31. I. A. Hassanien and R. S. R. Gorla, *Acta Mech.* 84, 191 **(1990)**.
32. A. Majeed, A. Zeeshan, S. Z. Alamri, and R. Ellahi, *Neural Com. Appl.* 30, 1947 **(2018)**.
33. A. Hussain, M. Y. Malik, M. Awais, T. Salahuddin, and S. Bilal, *Neural Comp. Appl.* 31, 425 **(2019)**.
34. Z. Shah, E. Bonyah, S. Islam, and W. Khan, Ishaq, *Heliyon* 4, e00825 **(2018)**.
35. Kh. Hosseinzadeh, F. Afsharpanah, S. Zamani, M. Gholinia, and D. D. Ganji, *Case Studies Therm. Eng.* 12, 228 **(2018)**.
36. M. Abdollahzadeh, A. A. Sedighi, and M. Esmailpour, *Journal of Nanofluids* 7, 149 **(2018)**.
37. S. Baag, S. R. Mishra, M. M. Hoque, and N. N. Anika, *Journal of Nanofluids* 7, 570 **(2018)**.
38. M. I. Afridi and M. Qasim, *Journal of Nanofluids* 7, 783 **(2018)**.
39. I. Shravani, D. Ramya, and S. Joga, *Journal of Nanofluids* 7, 862 **(2018)**.
40. P. Nagasantoshi, G. V. Reddy, M. G. Reddy, and P. Padma, *Journal of Nanofluids* 7, 821 **(2018)**.
41. F. Ayodeji, A. Tope, and O. Samuel, *Amer. J. Mech. Indus. Eng.* 4, 86 **(2019)**.
42. B. Ramadevi, K. A. Kumar, and V. Sugunamma, *J. Thermal Anal. Calorimetry* 139, 1379 **(2020)**.
43. M. A. Ibrahim, G. A. Ahmed, M. Osman, L. A. Lund, M. B. Ayed, H. Belmabrouk, and I. Tlili, *Symmetry* 11, 297 **(2019)**.
44. F. Faraz, S. Haider, and S. M. Imran, *SN Applied Sciences* 2, 14 **(2020)**.
45. N. C. Rosca and I. Pop, *Europ. J. Mech.-B/Fluids* 51, 61 **(2015)**.
46. M. Naveed, Z. Abbas, and M. Sajid, *J. Appl. Fluid Mech.* 9, 131 **(2016)**.
47. Z. Abbas, M. Naveed, and M. Sajid, *J. Molec. Liquids* 215, 756 **(2016)**.
48. M. Imtiaz, T. Hayat, A. Alsaedi, and A. Hobiny, *J. Molec. Liquids* 221, 245 **(2016)**.
49. K. A. Kumar, V. Sugunamma, and N. Sandeep, *J. Therm. Anal. Calorimetry* 140, 1 **(2019)**.
50. T. Muhammad, K. Rafique, M. Asma, and M. Alghamdi, *Physica A: Stat. Mech. Appl.* 556, 123968 **(2020)**.
51. S. Ahmad, S. Nadeem, and N. Muhammad, *Commun. Theor. Phys.* 71, 344 **(2019)**.